ResearchGate

See discussions, stats, and author profiles for this publication at: https://www.researchgate.net/publication/51525227

Syntheses, Electrochemistry, and Photodynamics of Ferrocene–Azadipyrromethane Donor–Acceptor Dyads and Triads

ARTICLE *in* THE JOURNAL OF PHYSICAL CHEMISTRY A · AUGUST 2011

Impact Factor: 2.69 · DOI: 10.1021/jp205236n · Source: PubMed

CITATIONS
35

READS
36

7 AUTHORS, INCLUDING:

Mohamed E El-Khouly
Kafrelsheikh University
129 PUBLICATIONS **3,118** CITATIONS
SEE PROFILE

Navaneetha K Subbaiyan
Los alamos national lab
46 PUBLICATIONS **1,504** CITATIONS
SEE PROFILE

Melvin E Zandler
Wichita State University
106 PUBLICATIONS **3,289** CITATIONS
SEE PROFILE

Mustafa Supur
University of Alberta
20 PUBLICATIONS **223** CITATIONS
SEE PROFILE

Available from: Mohamed E El-Khouly
Retrieved on: 17 January 2016

THE JOURNAL OF PHYSICAL CHEMISTRY A

ARTICLE

pubs.acs.org/JPCA

Syntheses, Electrochemistry, and Photodynamics of Ferrocene−Azadipyrromethane Donor−Acceptor Dyads and Triads

Anu N. Amin,[†] Mohamed E. El-Khouly,[§] Navaneetha K. Subbaiyan,[‡] Melvin E. Zandler,[†] Mustafa Supur,[§] Shunichi Fukuzumi,[*,∥,†] and Francis D'Souza[*,†,‡]

[†]Department of Chemistry, Wichita State University, Wichita, Kansas 67260-0051, United States

[‡]Department of Chemistry, University of North Texas, 1155 Union Circle, #305070, Denton, Texas 76203-5017, United States

[§]Graduate School of Engineering, Osaka University, ALCA, Japan Science and Technology Agency (JST), Suita, Osaka 565-0871, Japan

[∥]Department of Bioinspired Science, Ewha Womans University, Seoul, 120-750, Korea

Supporting Information

ABSTRACT: A near-IR-emitting sensitizer, boron-chelated tetraarylazadipyrromethane, has been utilized as an electron acceptor to synthesize a series of dyads and triads linked with a well-known electron donor, ferrocene. The structural integrity of the newly synthesized dyads and triads was established by spectroscopic, electrochemical, and computational methods. The DFT calculations revealed a 'molecular clip'-type structure for the triads wherein the donor and acceptor entities were separated by about 14 Å. Differential pulse voltammetry combined with spectroelectrochemical studies have revealed the redox states and estimated the energies of the charge-separated states. Free-energy calculations revealed the charge separation from the covalently linked ferrocene to the singlet excited ADP to yield $Fc^{+}-ADP^{\bullet-}$ to be energetically favorable. Consequently, the steady-state emission studies revealed quantitative quenching of the ADP fluorescence in all of the investigated dyads and triads. Femtosecond laser flash photolysis studies provided concrete evidence for the occurrence of photoinduced electron transfer in these donor−acceptor systems by providing spectral proof for formation of ADP radical anion ($ADP^{\bullet-}$) which exhibits a diagnostic absorption band in the near-IR region. The kinetics of charge separation and charge recombination measured by monitoring the rise and decay of the $ADP^{\bullet-}$ band revealed ultrafast charge separation in these molecular systems. The charge-separation performance of the triads with two ferrocenes and a fluorophenyl-modified ADP macrocycle was found to be superior. Nanosecond transient absorption studies revealed the charge-recombination process to populate the triplet ADP as well as the ground state.

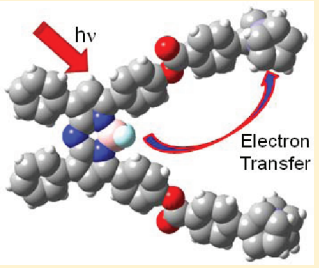

1. INTRODUCTION

Porphyrins and phthalocyanines have extensively been used as light-harvesting and electron-transfer units in artificial photosynthetic systems performing photoinduced energy and electron transfer,[1−6] because the photosynthetic reaction center includes the porphyrin derivatives, i.e., bacteriochlorophylls, which act as light-harvesting antenna and electron donors in the electron-transfer cascade. On the other hand, boron dipyrromethene (BODIPY) fluorophores, which are derived from 4,4-difluoro-1,3,5,7-tetramethyl-4-bora-3a,4adiaza-*s*-indacene,[7] have also been widely employed as light-harvesting antenna and electron donor or acceptor as well as laser dyes in a variety of applications, because a large number of BODIPY derivatives are readily obtained by modification at carbon positions at 1, 3, 5, 7, and 8,[8,9] exhibiting attractive photophysical characteristics with strong absorption bands in the visible region, which are comparable to those of porphyrins.[10−17]

Aza−BODIPY dyes (abbreviated as ADP), with a nitrogen in position 8 instead of the carbon in C8 BODIPY, have attracted increasing attention, because ADPs show high extinction coefficients ($7-8 \times 10^5$ M^{-1} cm^{-1}), large fluorescence quantum yields beyond 700 nm, and a less negative one-electron reduction potential.[18,19] Consequently, they have been used in applications involving development of sensors and photodynamic therapy agents.[20,21] In addition, as demonstrated here, the electron-transfer dynamics can be readily monitored, because the one-electron-reduced product exhibits a near-IR band beyond 800 nm, sufficiently far from the spectral region of the triplet−triplet absorption of most of the sensitizers. However, their application in light-energy-harvesting donor−acceptor systems has yet to be explored.[22]

We report herein the utility of ADP derivatives as a light-harvesting unit as well as an electron acceptor unit in a series of newly synthesized dyads and triads featuring ferrocene as an electron donor (Scheme 1). In the first type, ADP is linked to one or two ferrocene units (Fc−ADP and Fc_2−ADP), while in the second type, two 4-fluorobenzenes instead of the phenyl rings are substituted to introduce additional electron deficiency of the ADP macrocycle (Fc−$ADPF_2$ and Fc_2−$ADPF_2$). Compounds ADP, $ADP(OH)_2$, and $ADPF_2(OH)_2$ were also synthesized as control compounds. Efficient photoinduced electron transfer has

Received: June 3, 2011
Revised: July 16, 2011
Published: July 27, 2011

ACS Publications © 2011 American Chemical Society

Scheme 1. Structures of Newly Synthesized Ferrocene−ADP Dyads and Triads in the Present Study

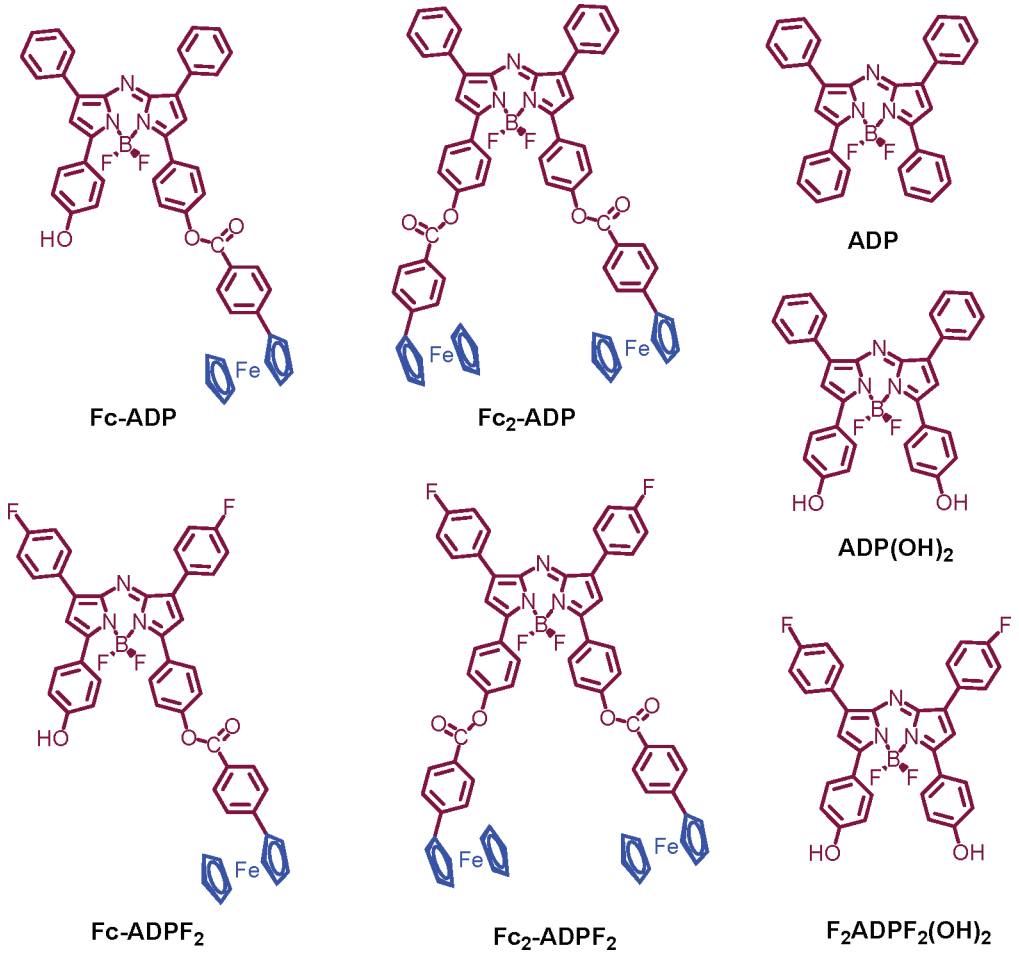

been witnessed in these donor−acceptor dyads and triads by femtosecond laser flash photolysis measurements.

2. RESULTS AND DISCUSSION

2.1. Syntheses of Ferrocene−ADP Dyads and Triads. The syntheses of the donor−acceptor systems involved a multistep approach as shown in Scheme 2, and the details are given in the Experimental Section. Briefly, 1-(4-hydroxyphenyl)-3-phenylpropenone (**1a**) and 1-(4-hydroxyphenyl)-3-(4-fluorophenyl)-propenone (**1b**) were synthesized from a reaction of the corresponding benzaldehyde, 4-hydroxyacetophenone, and potassium hydroxide. These compounds were subsequently reacted with nitromethane and diethylamine in dry ethanol to obtain respective 1-(4-hydroxyphenyl)-4-nitro-3-phenylbutan-1-one (**2a**) and 1-(4-hydroxyphenyl)-4-nitro-3-(4-fluorophenyl)butan-1-one (**2b**). The [5-(4-hydroxyphenyl)-3-phenyl-1*H*-pyrrol-2-yl]-[5-(4-hydroxyphenyl)-3-phenylpyrrol-2-ylidene]amine (**3a**) and [5-(4-hydroxyphenyl)-3-(4-fluorophenyl)-1*H*-pyrrol-2-yl]-[5-(4-hydroxyphenyl)-3-(4-fluorophenyl)pyrrol-2-ylidene]amine (**3b**) were synthesized by reactions of **2a** and **2b** with ammonium acetate in ethanol. Next, the BF_2 chelate of [5-(4-hydroxyphenyl)-3-phenyl-1*H*-pyrrol-2-yl]-[5-(4-hydroxyphenyl)-3-phenylpyrrol-2-ylidene]amine (**4a**) and BF_2 chelate of [5-(4-hydroxyphenyl)-3-(4-fluorophenyl)-1*H*-pyrrol-2-yl]-[5-(4-hydroxyphenyl)-3-(4-fluorophenyl)pyrrol-2-ylidene]amine (**4b**) were synthesized by reactions of **3a** and **3b** with diisopropylethylamine and boron trifluoride diethyl etherate in dry CH_2Cl_2. Finally, the ferrocene−ADP dyads and triads were obtained by reactions of **4a** and **4b** with appropriate amounts of 4-ferrocenylbenzoic acid in the presence of EDCl followed by chromatographic purification. The structural integrity of the newly synthesized compounds was established from ^{1}H NMR, mass, and optical techniques (see Figures S1−S7, Supporting Information).

2.2. Steady-State Absorption and Fluorescence Measurements. Figure 1a and 1b shows the absorption spectra of the investigated compounds in benzonitrile. The most intense band of ADP was located in the range 665−700 nm depending upon the substituents on the aromatic rings. A less intense band in the 465−485 nm region was also observed. The near-IR band was red shifted by about 150 nm compared to the BODIPY derivatives,[16,17] which suggests its usefulness in light-harvesting system. Interestingly, the dihydroxy derivatives, **4a** and **4b**, revealed significant bathochromic shifts, suggesting a significant influence of the hydroxyl groups. However, the presence of fluoro groups on the phenyl rings had virtually no influence on the optical behavior. In the allowed wavelength range of the benzonitrile solvent and due to the low molar extinction coefficient, the absorbance band corresponding to ferrocene was also not observed.

As shown in Figure 1c and 1d, ADP revealed a single fluorescence band at 682 nm while the dihydroxy derivatives (**4a** and

Scheme 2. Synthetic Procedure Adapted for Ferrocene−ADP Dyads and Triads

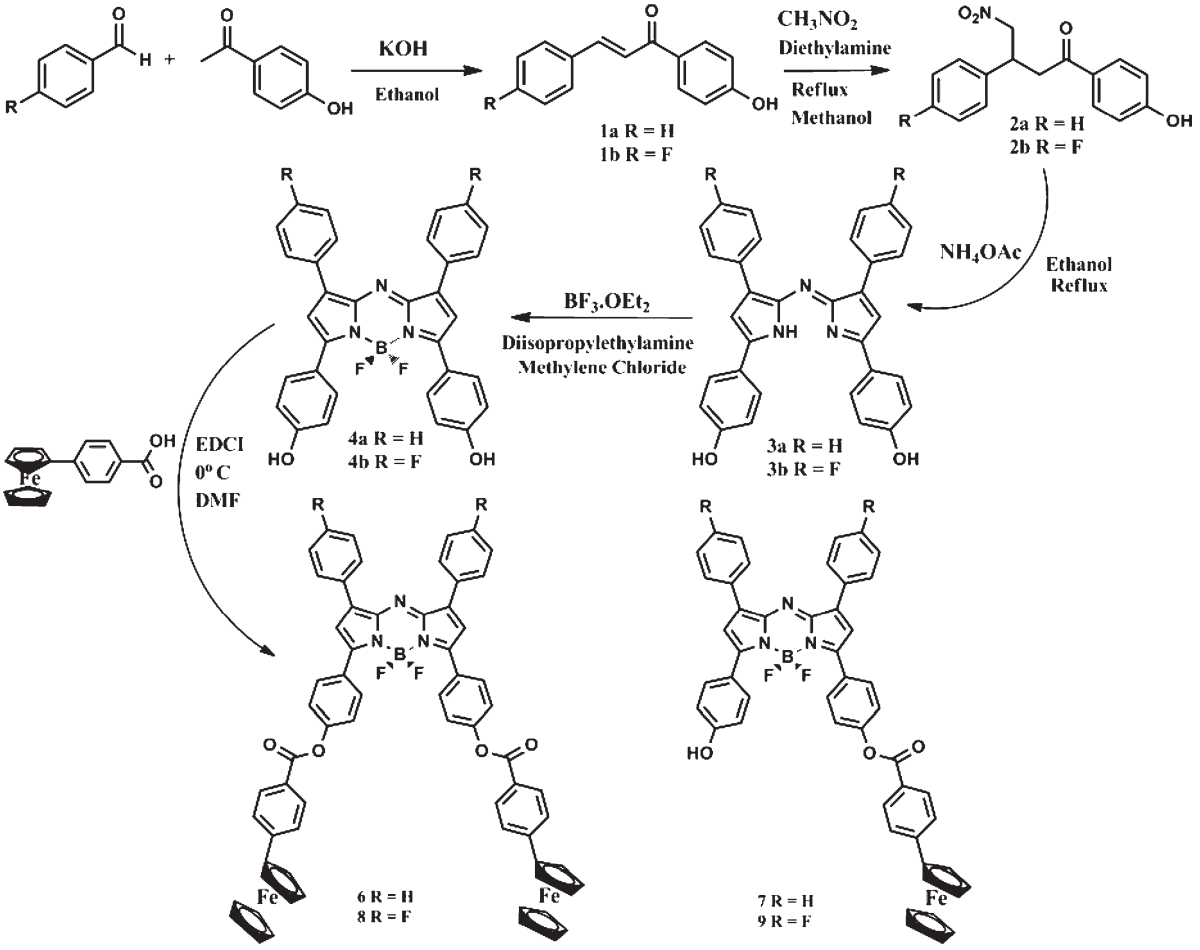

4b) revealed a red-shifted band located at 730 nm. The presence of ferrocene entities for both dyads and triads quantitatively quenched the fluorescence, suggesting the occurrence of photochemical events from the singlet excited ADP. The fluorescence quantum yields of Fc−ADP ($\Phi_f = 5 \times 10^{-3}$) and Fc_2−ADP ($\Phi_f = 2 \times 10^{-3}$) were found to be much smaller than that of ADP reference ($\Phi_f = 0.13$).

2.3. Electrochemistry, Spectroelectrochemistry, and Energy Levels. In order to establish the energy levels and spectral characterization of electroreduced ADP, electrochemical studies using differential pulse voltammetry and spectroelectrochemical studies were performed. Figure 2 shows differential pulse voltammograms (DPVs) of the dyads and triads along with the control compounds in benzonitrile, 0.1 M (n-Bu_4N)ClO_4, while the redox data are summarized in Table 1. ADP revealed both one-electron reduction and one-electron oxidation processes located at −0.79 and 0.80 V vs Fc/Fc^+, respectively. The first reduction was found to be cathodically shifted by nearly 200 mV compared with the well-known electron acceptor, C_{60}.[23] Introducing the hydroxyphenyl groups on ADP caused the reduction harder by about 100 mV, while the oxidation process was irreversible (from cyclic voltammetric experiments), however, with cathodically shifted potentials. In contrast, the added fluorophenyl entities in $ADPF_2(OH)_2$ derivative had little or no effect on the reduction potentials compared with the reduction potentials of the corresponding $ADP(OH)_2$.

In the dyads Fc−ADP and Fc−$ADPF_2$, the ferrocene oxidation occurred at around 0.07 V vs Fc/Fc^+, which is about 70−80 mV anodically shifted as compared with pristine ferrocene oxidation that could easily be attributed to chemical functionalization of the ferrocene entity.[24] The first reduction potential of ADP macrocycle was located at −0.84 V vs Fc/Fc^+; the fluorine entities had no effect on the reduction potential of the dyad. However, compared with pristine ADP reduction, these reductions were cathodically shifted by 50 mV. In the case of triads, the current for ferrocene oxidation was twice as much as that of ADP reduction, and the potentials for ferrocene oxidation were close to that observed for the corresponding dyads, while the reduction potentials were close to that of pristine ADP. These results collectively suggest ferrocene is electron rich and ADP is an electron-deficient entity of the dyad.[25] Since there were no appreciable changes in the oxidation potentials of the ferrocene entity in the dyads and triads, the absence of inter- or intramolecular interactions could be envisioned. The energies of the charge-separated states were calculated using the redox, geometric, and optical data according to Weller's approach,[26] and the calculated values are given in Table 1. By comparing these energy levels of the charge-separated states with the energy levels of the excited states, the driving forces of charge separation (ΔG^S_{CS}) were also evaluated. Generation of Fc^+−$ADP^{\bullet-}$ for the dyad and Fc^+Fc−$ADP^{\bullet-}$ for the triad was found to be exergonic via the singlet excited state of ADP in benzonitrile.

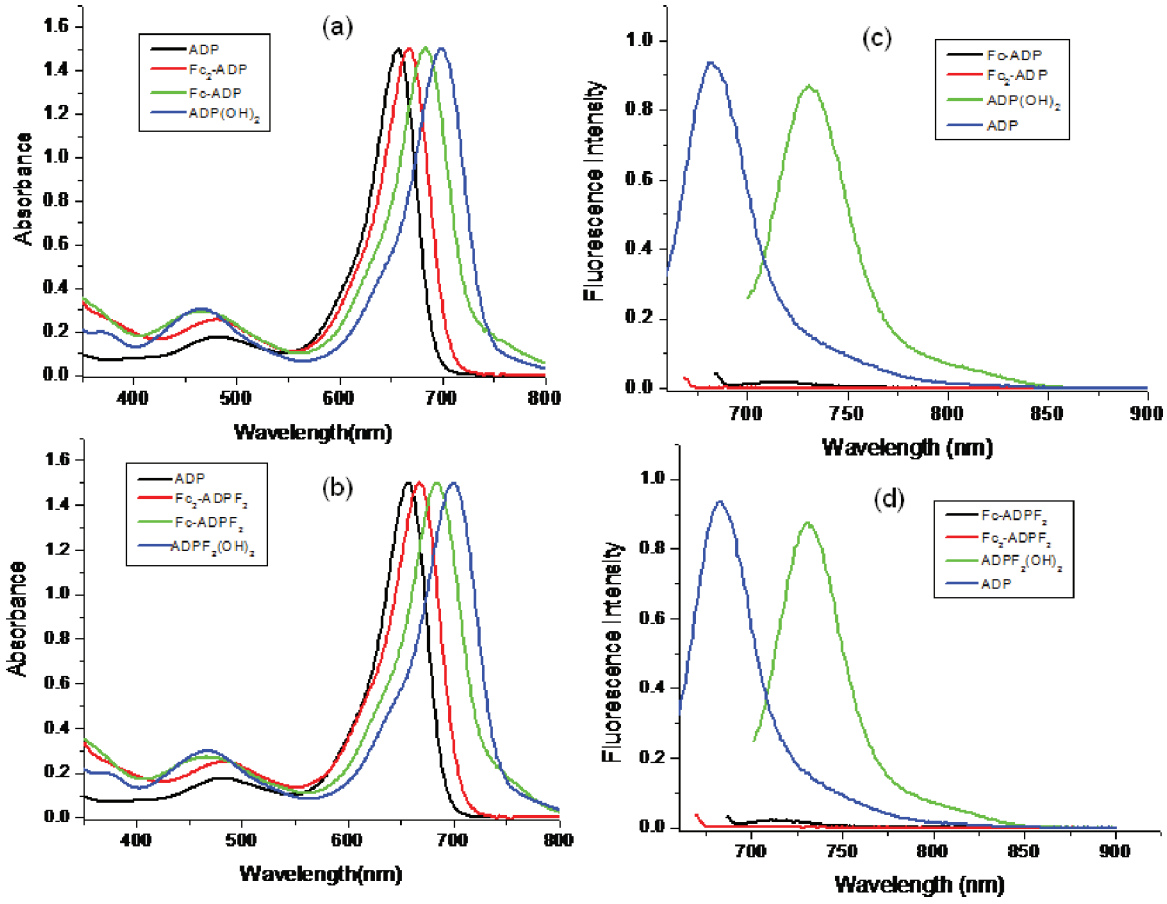

Figure 1. Absorbance spectra (a and b) and emission spectra (c and d) of the indicated compounds (8.0 μM) in benzonitrile (see Scheme 1 for abbreviated structures). The compounds were excited at the corresponding near-IR peak maxima of the ADP macrocycle.

Facile reduction of ADP prompted us to perform spectroelectrochemical studies to characterize the one-electron-reduced product. Figure 3 shows the spectral changes recorded during the course of the first reduction of ADP in benzonitrile, 0.1 M (n-Bu_4N)ClO_4, in a thin-layer spectroelectrochemical cell. During the course of reduction, the peak located at 658 nm diminished in intensity with the concurrent appearance of new bands at 446 and 820 nm. This process was reversible, that is, switching the potential to 0.0 V resulted in recovery of the entire spectrum of the neutral ADP. The near-IR band at 820 nm $ADP^{\bullet-}$ is located sufficiently far from the spectral region of the triplet absorption of the donor and acceptor, serving as a diagnostic band to identity the electron-transfer products in photochemical electron-transfer reactions, and follows the kinetics of charge separation in the newly developed dyads.

Figure 4 shows the B3LYP/3-21G(*)-optimized structure and molecular electrostatic potential map (MEP) of a representative Fc_2−ADP triad.[27,28] The structure was completely optimized on a Born−Oppenheimer potential energy surface. The ADP segment was found to be flat, while the peripheral aromatic rings were slightly tilted as evidenced by a dihedral angle of 22−29° to the ADP ring atoms. The two ferrocene entities linked to ADP formed a 'molecular clip'-type structure in which the distance between the boron of ADP to the iron of ferrocene was 14.1 Å while the distance between the closest carbon of ADP to the closet carbon of ferrocene was 12.1 . The Fe−Fe distance between the two ferrocene entities was 15.0 Å, while the angle between Fe−B−Fe was 63°. The MEP diagram also suggested the electron-deficient nature of the ADP unit of the triad.

2.4. Photodynamics Studies. Femtosecond and nanosecond laser flash photolysis techniques were used to investigate photodynamics of the dyads and triads. Figures 5 and S8, Supporting Information, show the transient spectral response for representative dyads and triad. In all of these systems, fast growth of bands corresponding to $ADP^{\bullet-}$ were observed in the 440 and 820 nm region,[22] confirming charge separation. The observed absorption bands at 440 and 820 nm were assigned to $ADP^{\bullet-}$ by comparison with those of $ADP^{\bullet-}$ produced either by spectroelectrochemistry studies (Figure 3) or by the one-electron reduction of ADP with tetrakis(dimethylamino)ethylene (Figure S9 in the Supporting Information). The bands corresponding to Fc^+ were not observed due to its low molar extinction coefficient. The rate constants of the charge separation (k^S_{CS}) and the charge recombination (k_{CR}) were evaluated by monitoring the rise and decay of the 820 nm band, and such data are given in Table 2. The fast and efficient charge separation in the investigated dyads ($\sim 10^{12}$ s^{-1}) suggests that the CS process is located at the top of the normal region of the Marcus parabola.[29] The k^S_{CR} values are found to be considerably smaller than k^S_{CS}, suggesting that the CR processes are located at the upward of the inverted region of the Marcus parabola ($-\Delta G_{CR}$ = 0.98 eV).[29−31] For a given series of triads (fluorinated or nonfluorinated), the k^S_{CS} values were slightly larger for the triads. Between fluorinated and nonfluorinated ADPs, the k^S_{CS} values were slightly higher for the fluorinated

dx.doi.org/10.1021/jp205236n |J. Phys. Chem. A 2011, 115, 9810–9819

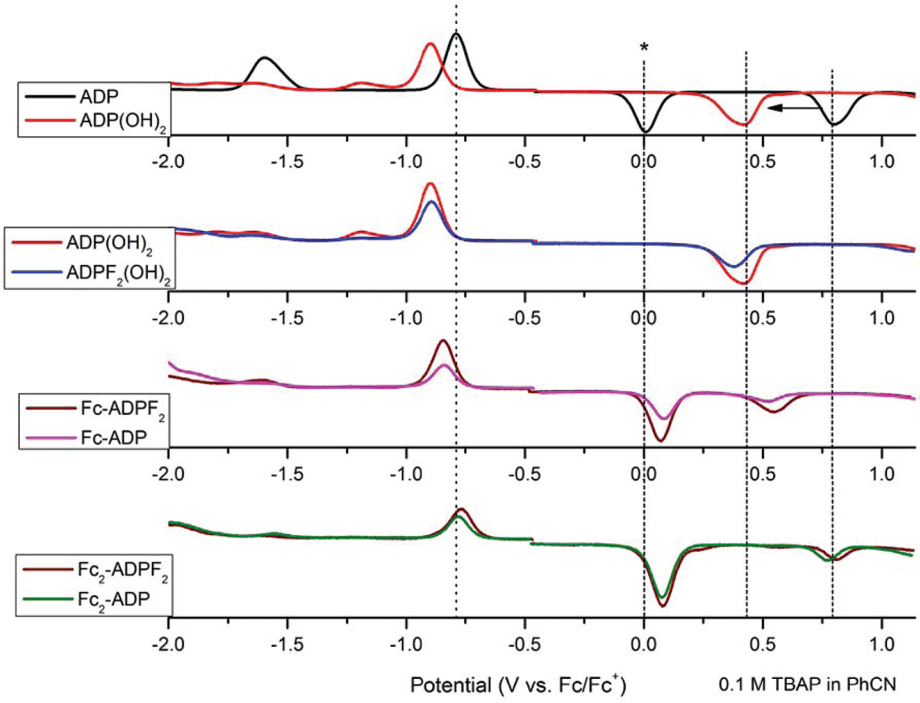

Figure 2. Differential pulse voltammograms of the indicated compounds (see Scheme 1 for structures) in benzonitrile, 0.1 M (n-Bu_4N)ClO_4. Scan rate = 5 mV/s, pulse width = 0.25 s, pulse height = 0.025 V. The asterisk in the top panel shows the oxidation process of ferrocene used as an internal standard.

Table 1. Electrochemical Redox Potentials (V vs Fc/Fc^+), Energy Levels of the Charge-Separated States (ΔG_{CR}), and Free-Energy Changes for Charge Separation (ΔG^S_{CS}) for the Ferrocene−ADP Dyads and Triads in Benzonitrile

compound	$Fc^{0/+}$/V	$ADP^{0/\bullet-}$/V	$ADP^{0/\bullet+}$/V	$-\Delta G_{CR}{}^a$/eV	$-\Delta G^S_{CS}{}^b$/eV
ADP		−0.79	0.80		
$ADP(OH)_2$		−0.90	0.42		
$ADPF_2(OH)_2$		−0.89	0.38		
Fc−ADP	0.08	−0.84	0.52	0.98	0.87
Fc_2−ADP	0.07	−0.78	0.77	0.91	0.94
Fc−$ADPF_2$	0.07	−0.84	0.55	0.97	0.88
Fc_2−$ADPF_2$	0.08	−0.76	0.81	0.91	0.94

[a] $-\Delta G_{CR} = e(E_{ox} - E_{red}) + \Delta G_S$, where $\Delta G_S = -e^2/(4\pi\varepsilon_0\varepsilon_R R_{Ct\text{-}Ct})$ and ε_0 and ε_R refer to the vacuum permittivity and dielectric constants of benzonitrile. [b] $-\Delta G^S_{CS} = \Delta E_{0-0} - (-\Delta G_{CR})$, where ΔE_{0-0} is the energy of the lowest excited states of ADP being 1.85 eV in benzonitrile.

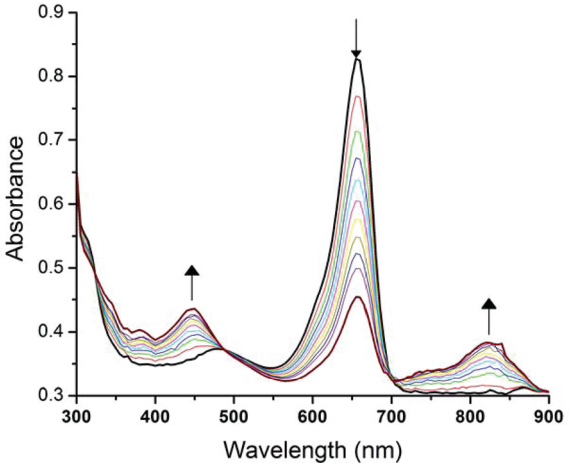

Figure 3. Spectral changes observed during the first reduction of ADP in benzonitrile containing 0.10 M (n-Bu_4N)ClO_4 using a thin-layer spectroelectrochemical cell. Potential applied was −0.80 V vs Fc/Fc^+.

dyads and triads. Interestingly, the k_{CR} values were larger for the triads compared with the dyads. The figure of merit for charge stabilization, k^S_{CS}/k_{CR}, was also evaluated as given in Table 2. Such data indicate moderate amounts of charge stabilization in these systems and better values for the dyads compared to the triads.

Nanosecond transient absorption spectra were recorded to probe the fate of charge-separated species. As shown in Figures 6 and S10, Supporting Information, nanosecond transient absorption spectra of pristine ADP, Fc−ADP dyad, and Fc_2−ADP triad revealed a broad band in the 400−550 nm region corresponding to the triplet excited state of ADP (^{3}ADP*). From these observations, one could see the enhancement of the ^{3}ADP* formation in the case of dyad and triad compared to pristine ADP. From the fitting of the transient band at 440 nm, the decay rate constants of the triplet ADP (k_T) were found to be 1.5×10^4, 2.0×10^6, and 2.1×10^7 s^{-1} for the ^{3}ADP*, Fc−^{3}ADP* dyad, and Fc_2−^{3}ADP* triad, respectively. The faster k_T of Fc−^{3}ADP* and Fc_2−^{3}ADP* compared to that of ^{3}ADP* may arise from quenching of the triplet ADP by the attached Fc entities. It is obvious that quenching of the triplet ADP increases with increasing the number of Fc entities.

As depicted in Figure 7, the charge-separation process from the Fc moiety to ^{1}ADP* takes place quite efficiently, leading to formation of the charge-separated state (Fc^+−$ADP^{\bullet-}$) in benzonitrile. The formed charge-separated states decayed with lifetimes of 10−27 ps to populate the ADP

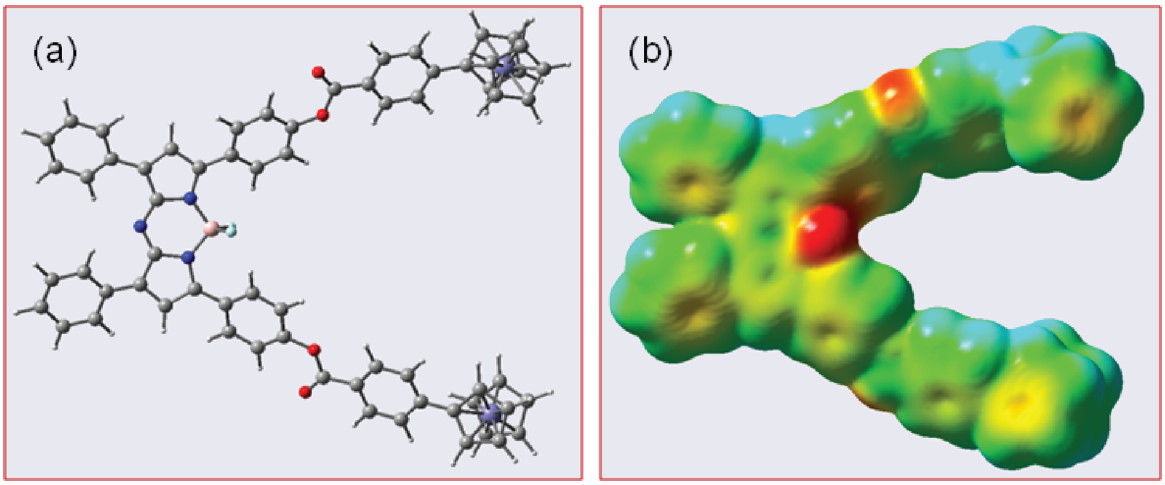

Figure 4. (a) B3LYP/3-21G(*)-optimized structure and (b) molecular electrostatic potential map of the Fc_2—ADP triad.

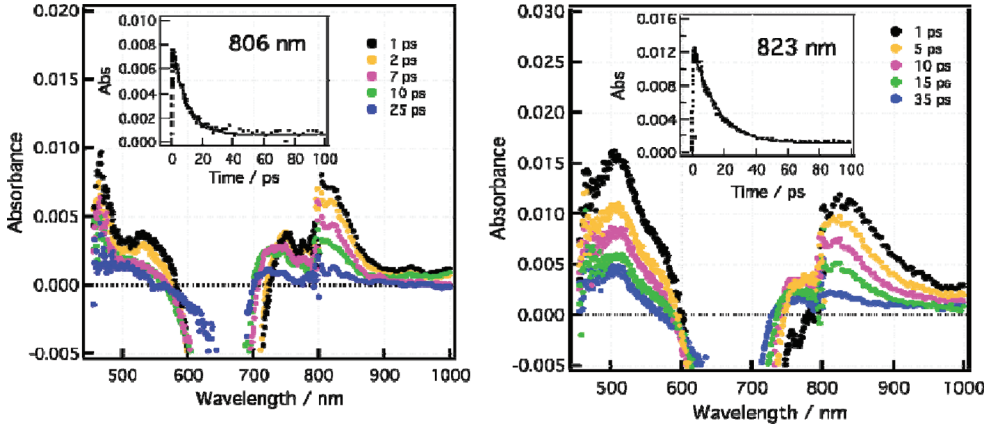

Figure 5. Femtosecond transient absorption spectral traces at different time intervals for Fc—ADP (left) and Fc_2—ADP (right) in benzonitrile; λ_{ex} = 440 nm. The figure inset shows decay of the transient band corresponding to ADP radical anion.

Table 2. Charge-Separation (k^S_{CS}) and Charge-Recombination Rate Constants (k_{CR}) and Singlet Excited States of ADP for the Ferrocene—ADP Donor—Acceptor Systems in Benzonitrile

compound	k^S_{CS}/s^{-1}	k_{CR}/s^{-1}	k^S_{CS}/k_{CR}
Fc—ADP	1.1×10^{12}	6.8×10^{10}	16
Fc_2—ADP	1.1×10^{12}	1.1×10^{11}	10
Fc—$ADPF_2$	1.7×10^{12}	6.1×10^{10}	27
Fc_2—$ADPF_2$	2.3×10^{12}	1.4×10^{11}	17

ground state as well as the low-lying ADP triplet state (<1 eV),[32] which in turn was quenched by the attached Fc and decayed to its ground state.

3. CONCLUSIONS

A series of ferrocene—ADP dyads and triads has been newly synthesized to probe the electron-acceptor behavior of the near-IR-emitting sensitizer, boron-chelated tetraarylazadipyrromethane (ADP). The multistep synthesis yielded the desired dyads and triads whose structural integrity was established using spectroscopic, electrochemical, and computational methods. A 'molecular clip'-type structure for the triads was envisioned from computational energy minimization calculations involving DFT methods. The redox potentials and site of electron transfer were established from electrochemical and spectroelectrochemical studies. Free-energy calculations revealed charge separation from the covalently linked ferrocene to the singlet excited ADP to yield the charge-separated state (Fc^+—$ADP^{\bullet-}$) to be energetically favorable. Steady-state emission and femtosecond laser flash photolysis studies provided tangible evidence for the occurrence of photoinduced electron transfer in these donor—acceptor systems by providing a spectral signature for $ADP^{\bullet-}$ formation in the near-IR region. The kinetics of the charge separation and charge recombination evaluated from femtosecond laser flash photolysis studies revealed fast and efficient charge separation in these molecular systems. Nanosecond transient absorption studies revealed the charge-recombination process to populate the triplet ADP as well as the ADP ground state. The present study successfully demonstrates utilization of a near-IR-absorbing sensitizer, boron-chelated tetraarylazadipyrromethane, as a suitable candidate to build new types of

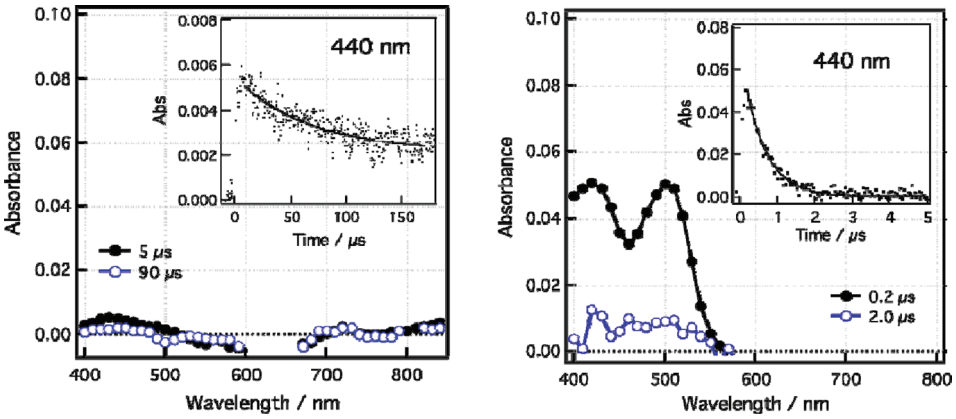

Figure 6. Nanosecond transient absorption spectra of ADP (left) and Fc−ADP (right) in benzonitrile; λ_{ex} = 475 nm. The figure inset shows decay of the 440 nm transient band corresponding to ^{3}ADP*.

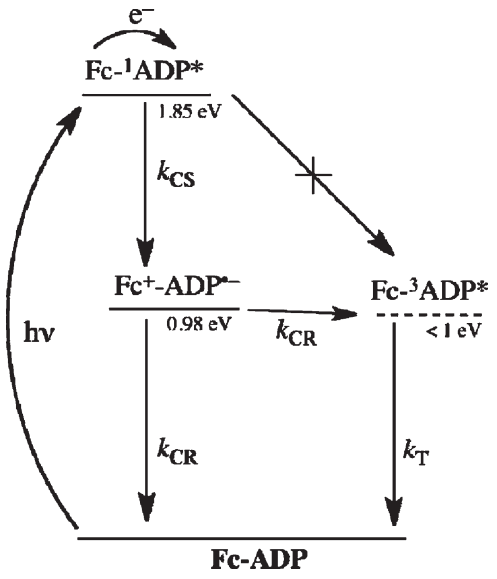

Figure 7. Energy-level diagram of photoinduced intramolecular events of Fc−ADP in benzonitrile.

donor−acceptor dyads and triads for light-energy-harvesting-related applications. Further studies along this line are in progress in our laboratories.

4. EXPERIMENTAL SECTION

Chemicals. All reagents were from Aldrich Chemicals (Milwaukee, WI), while the bulk solvents utilized in the syntheses were from Fischer Chemicals. Tetra-*n*-butylammonium perchlorate, $(n\text{-}Bu_4N)ClO_4$, used in electrochemical studies was from Fluka Chemicals. The initial synthesis of ADP macrocycle was performed according to the procedure reported by O'Shea and co-workers[12] by needed modifications.

Preparation of 1-(4-Hydroxyphenyl)-3-phenylpropenone (1a). Benzaldehyde (2.1 g, 2×10^{-2} mol), 4-hydroxy acetophenone (2.69 g, 2×10^{-2} mol), and potassium hydroxide (0.03 g, 6×10^{-4} mol) were dissolved in ethanol/water (85:15 v/v, 100 mL) and stirred at room temperature for a period of 24 h. The reaction mixture was allowed to cool in an ice−water bath during which the product precipitated. Filtration of the reaction mixture gave a pale white solid product (85% yield, 3.81 g). ^{1}H NMR (300 MHz, $CDCl_3$): δ = 7.99−8.04 (m, 2H), 7.77−7.84 (m, 1H), 7.60−7.68, (m, 2H), 7.5−7.58 (m, 1H), 7.39−7.45 (m, 3H), 6.9−6.97 (m, 2H) ppm.

Preparation of 1-(4-Hydroxyphenyl)-3-(4-fluorophenyl)-propenone (1b). 4-Fluorobenzaldehyde (2.5 g, 2×10^{-2} mol), 4-hydroxy acetophenone (2.74 g, 2×10^{-2} mol), and potassium hydroxide (0.03 g, 6×10^{-4} mol) were dissolved in ethanol/water (85:15 v/v, 100 mL) and stirred at room temperature for a period of 24 h. The reaction mixture was allowed to cool in an ice−water bath during which the product precipitated. Filtration of the reaction mixture gave a yellow solid product (85%, yield, 4.14 g). ^{1}H NMR (300 MHz, $CDCl_3$): δ = 7.95−8.03 (m, 2H), 7.7−7.8 (m, 1H), 7.58−7.66, (m, 2H), 7.4−7.48 (m, 1H), 7.05−7.14 (m, 2H), 6.87−6.93 (m, 2H) ppm.

Preparation of 1-(4-Hydroxyphenyl)-4-nitro-3-phenylbutan-1-one (2a). 1-(4-Hydroxyphenyl)-3-phenyl propenone (5.0 g, 2.2×10^{-2} mol), nitromethane (13.61 g, 0.223 mol), and diethylamine (8.12 g, 0.111 mol) were dissolved in dry ethanol (35 mL) and heated under reflux for 24 h. The solution was cooled and acidified with 1 M HCl to precipitate the compound (72% yield, 4.58 g). ^{1}H NMR (300 MHz, $CDCl_3$): δ = 7.82 (d, J = 8.48 Hz, 2H), 7.2−7.34 (m, 5H), 6.8 (d, J = 8.5 Hz, 2H), 4.8−4.83 (m, 1H), 4.62−4.7 (m, 1H), 4.15−4.2 (m, 1H), 3.35−3.4 (m, 2H) ppm.

Preparation of 1-(4-Hydroxyphenyl)-4-nitro-3-(4-fluorophenyl)butan-1-one (2b). 1-(4-Hydroxyphenyl)-3-(4-fluorophenyl)propenone (5.0 g, 2.1×10^{-2} mol), nitromethane (12.64 g, 0.207 mol), and diethylamine (7.53 g, 0.103 mol) were dissolved in dry ethanol (35 mL) and heated under reflux for 24 h. The solution was cooled and acidified with 1 M HCl to precipitate the compound (70% yield, 4.38 g). ^{1}H NMR (300 MHz, $CDCl_3$): δ = 7.80 (d, J = 8.4 Hz, 2H), 7.2 (m, 2H), 6.95−7.03 (m, 2H), 6.8 (d, J = 8.45 Hz, 2H), 4.75−4.82 (m, 1H), 4.6−4.67 (m, 1H), 4.14−4.21 (m, 1H), 3.3−3.38 (m, 2H) ppm.

Preparation of [5-(4-Hydroxyphenyl)-3-phenyl-1*H*-pyrrol-2-yl]-[5-(4-hydroxyphenyl)-3-phenylpyrrol-2-ylidene]amine (3a). 1-(4-Hydroxyphenyl)-4-nitro-3-phenylbutan-1-one (5 g, 1.8×10^{-2} mol), ammonium acetate (47.31 g, 0.61 mol), and ethanol (125 mL) were heated under reflux for 24 h. During the course of the reaction, the product precipitated as a blue-black solid. The reaction

was allowed to cool to room temperature, and solid was filtered and washed with ethanol to give the product (51% yield, 2.16 g). ^{1}H NMR (300 MHz, $CDCl_3$): δ = 8.04 (d, J = 6.62 Hz, 4H), 7.84 (d, 4H), 7.32−7.4 (m, 6H), 7.12 (s, 2H), 6.98 (d, J = 8.69 Hz, 4H) ppm.

Preparation of [5-(4-Hydroxyphenyl)-3-(4-fluorophenyl)-1*H*-pyrrol-2-yl]-[5-(4-hydroxyphenyl)-3-(4-fluorophenyl) pyrrol-2-ylidene]amine (3b). 1-(4-Hydroxyphenyl)-4-nitro-3-(4-fluorophenyl)butan-1-one (5 g, 1.6×10^{-2} mol), ammonium acetate (44.50 g, 0.58 mol), and ethanol (125 mL) were heated under reflux for 24 h. During the course of the reaction, the product precipitated as a blue-black solid. The reaction was allowed to cool to room temperature, and solid was filtered and washed with ethanol to give the product (51% yield, 2.18 g). ^{1}H NMR (300 MHz, $CDCl_3$): δ = 7.96−8.0 (m, 4H), 7.76 (d, J = 8.74 Hz, 4H), 7.0−7.08 (m, 6H), 6.92 (d, J = 8.73 Hz, 4H) ppm.

Preparation of BF_2 Chelate of [5-(4-Hydroxyphenyl)-3-phenyl-1*H*-pyrrol-2-yl]-[5-(4-hydroxyphenyl)-3-phenylpyrrol-2-ylidene]amine (4a). [5-(4-Hydroxyphenyl)-3-phenyl-1*H*-pyrrol-2-yl]-[5-(4-hydroxy-phenyl)-3-phenylpyrrol-2-ylidene]amine (1 g, 2.07 mmol) was dissolved in dry CH_2Cl_2 (100 mL). Diisopropylethylamine (2.71 g, 2.1×10^{-2} mol) and boron trifluoride diethyl etherate (4.16 g, 2.9×10^{-2} mol) were added, and the mixture was stirred at room temperature under N_2 for 24 h. The mixture was washed with water, and the organic layer was separated, dried over Na_2SO_4, and evaporated to dryness. The residue was purified by column chromatography on silica gel with CH_2Cl_2/ethyl acetate 4:1 to give metallic red solid (69% yield, 0.76 g). ^{1}H NMR (300 MHz, $CDCl_3$): δ = 8.1−8.15 (m, 8H), 7.35−7.45 (m, 6H), 7.18 (s, 2H), 6.9−6.93 (m, 4H) ppm. MS(MALDI-TOF); m/z $C_{32}H_{22}BF_2N_3O_2$ calcd, 529.18; found, 529.39.

Preparation of BF_2 Chelate of [5-(4-Hydroxyphenyl)-3-(4-fluorophenyl)-1*H*-pyrrol-2-yl]-[5-(4-hydroxyphenyl)-3-(4-fluorophenyl)pyrrol-2-ylidene]amine (4b). [5-(4-Hydroxyphenyl)-3-(4-fluoropheny)-1*H*-pyrrol-2-yl]-[5-(4-hydroxyphenyl)-3-(4-fluorophenyl)pyrrol-2-ylidene]amine (1 g, 1.93 mmol) was dissolved in dry CH_2Cl_2 (100 mL). Diisopropylethylamine (2.46 g, 1.9×10^{-2} mol) and boron trifluoride diethyl etherate (3.83 g, 2.7×10^{-2} mol) were added, and the mixture was stirred at room temperature under N_2 for 24 h. The mixture was washed with water, and the organic layer was separated, dried over Na_2SO_4, and evaporated to dryness. The residue was purified by column chromatography on silica gel with CH_2Cl_2/ethyl acetate 9:1 to give metallic red solid (48% yield, 0.524 g). ^{1}H NMR (300 MHz, $CDCl_3$): δ = 7.95−8.0 (m, 8H), 7.02−7.13 (m, 4H), 6.92 (s, 2H), 6.8−6.87 (m, 4H) ppm. MS(MALDI-TOF); m/z $C_{32}H_{20}BF_4N_3O_2$ calcd, 565.16; found, 565.45.

Preparation of 4-Ferrocenylbenzoic Acid (5). 4-Amino benzoic acid (7.0 g, 50 mmol), 80 mL of water, and 12 mL of concentrated hydrochloric acid was cooled to 0−5 °C in an ice bath. To this 20 mL of an aqueous solution of sodium nitrite was added dropwise with stirring; after further stirring it for 30 min the solution was kept under 5 °C for subsequent use. Ferrocene (10 g, 50 mmol) was dissolved in 100 mL of ethyl ether, 0.5 g of hexadecyltrimethylammonium bromide was added, and the mixture was cooled to 0−5 °C under stirring. To this the diazonium salt solution was added dropwise with stirring. The solution was then allowed to react for 2 h at room temperature. The ethyl ether was then rotary evaporated to give red solid. The solid was dissolved in 500 mL of water containing 5 g of NaOH at 90 °C and filtered while it was hot. The solid recovered was unreacted ferrocene. The filtrate was cooled, and the sodium salt of 4-ferrocenyl benzoic acid was precipitated. Filtration and acidification of the salt gave 4-ferrocenyl benzoic acid as a red solid (65% yield, 10.52 g). ^{1}H NMR (300 MHz, $CDCl_3$): δ = 7.9 (d, 2H), 7.2 (d, 2H), 4.7 (s, 2H), 4.3 (s, 2H), 4.02 (s, 5H).

Fc_2−ADP and Fc−ADP Triad and Dyad (6 and 7). 4-Ferrocenylbenzoic acid (200 mg, 0.7 mmol) was dissolved in 20 mL of DMF, to which EDCI (125.35 mg, 0.7 mmol) was added at 0 °C under N_2, followed by addition of compound **4a** (115.38 mg, 0.2 mmol), after which the mixture was stirred for 24 h. The mixture was washed with water, the organic layer was separated and dried over Na_2SO_4, and solvent was removed under reduced pressure. The residue was purified by column chromatography on silica gel with CH_2Cl_2:hexanes (1:1) to give compound **6** (6%, yield, 15 mg). ^{1}H NMR (400 MHz, $CDCl_3$): δ = 8.19−8.06 (m, 12H), 7.6 (d, J = 8.69 Hz, 4H), 7.53−7.43 (m, 6H), 7.4 (d, J = 8.94 Hz, 4H), 7.08 (s, 2H), 4.76 (t, 4H), 4.43 (t, 4H), 4.07 (s, 10H) ppm. MS (MALDI-TOF); $C_{66}H_{46}BF_2Fe_2N_3O_4$ calcd, 1105.22; found, 1105.22. Subsequent elution with CH_2Cl_2 gave compound **7** (21%, yield 38 mg). ^{1}H NMR (400 MHz, $CDCl_3$): δ = 8.17−8.03 (m, 10H), 7.52 (d, J = 8.6 Hz, 2H), 7.51−7.41 (m, 6H), 7.38 (d, J = 8.8 Hz, 2H), 7.1 (s, 1H), 6.97 (d J = 8.85 Hz, 3H), 4.78−4.75 (m, 2H), 4.45−4.42 (m, 2H), 4.07 (s, 5H) ppm. MS(MALDI-TOF); m/z: $C_{49}H_{34}BF_2FeN_3O_3$ calcd, 816.93; found, 817.20.

Fc_2−$ADPF_2$ and Fc−$ADPF_2$ Triad and Dyad (8 and 9). 4-Ferrocenylbenzoic acid (200 mg, 0.7 mmol) was dissolved in 20 mL of DMF, to which EDCI (125.35 mg, 0.7 mmol) was added at 0 °C under N_2, followed by addition of compound **4b** (123.23 mg, 0.2 mmol), after which the mixture was stirred for 24 h. The mixture was washed with water, the organic layer was separated and dried over Na_2SO_4, and solvent was removed under reduced pressure. The residue was purified by column chromatography on silica gel with CH_2Cl_2:hexanes (1:1) to give compound **8** (4% yield, 11 mg). ^{1}H NMR (400 MHz, $CDCl_3$): δ = 8.18−8.09 (m, 8H), 8.08−7.99 (m, 4H), 7.6 (d, J = 8.63, 4H), 7.4 (d, J = 8.86, 4H), 7.18 (m, 4H), 7.03 (s, 2H), 4.76 (t, 4H), 4.43 (t, 4H), 4.07 (s, 10H) ppm. MS (MALDI-TOF); $C_{66}H_{44}BF_4Fe_2N_3O_4$ calcd, 1141.21; found, 1141.00. Subsequent elution with CH_2Cl_2 yielded compound **9** (19% yield, 35 mg). ^{1}H NMR (400 MHz, $CDCl_3$): δ = 8.16−7.98 (m, 10H), 7.6 (d, J = 8.61 Hz, 2H), 7.38 (d, J = 8.87 Hz, 2H), 7.20−7.13 (m, 4H), 7.05 (s, 1H), 6.99−6.93 (m, 3H), 4.79−4.74 (m, 2H), 4.46−4.42 (m, 2H), 4.07 (s, 5H) ppm. MS(MALDI-TOF); m/z $C_{49}H_{32}BF_4FeN_3O_3$ calcd, 853.18; found, 852.70.

Spectral Measurements. UV−vis spectral measurements were carried out with a Shimadzu model 2550 double monochromator UV−visible spectrophotometer. The fluorescence emission was monitored using a Varian Eclipse spectrometer. A right angle detection method was used. ^{1}H NMR studies were carried out on a Varian 400 MHz spectrometer. Tetramethylsilane (TMS) was used as an internal standard. Differential pulse voltammograms were recorded on an EG&G PARSTAT electrochemical analyzer using a three-electrode system. A platinum button electrode was used as the working electrode. A platinum wire served as the counter electrode, and a Ag/AgCl electrode was used as the reference electrode. The ferrocene/ferrocenium redox couple was used as an internal standard. A homemade thin-layer spectroelectrochemical cell was used to record the spectral characteristics of reduced ADP. All solutions were purged prior to electrochemical and spectral measurements using argon gas. Matrix-assisted laser desorption/ionization time-of-flight mass spectra (MALDI-TOF) were measured on a Kratos Compact MALDI I (Shimadzu) for metal complex in PhCN with

dithranol used as a matrix. Computational calculations were performed by DFT B3LYP/3-21G* methods with the GAUSSIAN 03 software package[27] on high-speed PCs.

Laser Flash Photolysis. The studied compounds were excited by a Panther OPO pumped by a Nd:YAG laser (Continuum, SLII-10, 4−6 ns fwhm) with a power of 1.5 and 3.0 mJ per pulse. Transient absorption measurements were performed using a continuous xenon lamp (150 W) and an InGaAs-PIN photodiode (Hamamatsu 2949) as a probe light and a detector, respectively. The output from the photodiodes and a photomultiplier tube was recorded with a digitizing oscilloscope (Tektronix, TDS3032, 300 MHz). Femtosecond transient absorption spectroscopy experiments were conducted using an ultrafast source, Integra-C (Quantronix Corp.), an optical parametric amplifier, TOPAS (Light Conversion Ltd.), and a commercially available optical detection system, Helios provided by Ultrafast Systems LLC. The source for the pump and probe pulses were derived from the fundamental output of Integra-C (780 nm, 2 mJ/pulse and fwhm =130 fs) at a repetition rate of 1 kHz. Seventy five percent of the fundamental output of the laser was introduced into TOPAS, which has optical frequency mixers resulting in tunable range from 285 to 1660 nm, while the rest of the output was used for white light generation. Typically, 2500 excitation pulses were averaged for 5 s to obtain the transient spectrum at a set delay time. Kinetic traces at appropriate wavelengths were assembled from the time-resolved spectral data. All measurements were conducted at 298 K. Transient spectra were recorded using fresh solutions in each laser excitation.

■ ASSOCIATED CONTENT

Supporting Information. MALDIi-mass spectra of the investigated compounds, transient absorption spectrum of ADP in benzonitrile, and absorption spectra of $ADP^{\bullet-}$. This material is available free of charge via the Internet at http://pubs.acs.org.

■ AUTHOR INFORMATION

Corresponding Author

*E-mail: Francis.DSouza@UNT.edu (F.D.); Fukuzumi@chem.eng.osaka.u.ac.jp (S.F.).

■ ACKNOWLEDGMENT

This work was supported by the National Science Foundation (Grant No. 0804015 to F.D.), Flossie West Foundation, a Grant-in-Aid (Nos. 20108010 and 21750146), and the Global COE (center of excellence) program "Global Education and Research Center for Bio-Environmental Chemistry" of Osaka University from Ministry of Education, Culture, Sports, Science and Technology, Japan, KOSEF/MEST through WCU project (R31-2008-000-10010-0) from Korea.

■ REFERENCES

(1) (a) Gust, D.; Moore, T. A.; Moore, A. L. *Acc. Chem. Res.* **2009**, *42*, 1890–1898. (b) Gust, D.; Moore, T. A.; Moore, A. L. *Acc. Chem. Res.* **2001**, *34*, 40–48.(c) Gust, D.; Moore, T. A. In *The Porphyrin Handbook*; Kadish, K. M., Smith, K. M., Guilard, R., Eds.; Academic Press: San Diego, CA, 2000; Vol. 8, pp 153−190.

(2) (a) Wasielewski, M. R. *Acc. Chem. Res.* **2009**, *42*, 1910–1921. (b) Wasielewski, M. R. *Chem. Rev.* **1992**, *92*, 435–461.

(3) (a) de la Torre, G.; Vazquez, P.; Agullo-Lopez, F.; Torres, T. *Chem. Rev.* **2004**, *104*, 3723–3750. (b) Bottari, G.; de la Torre, G.; Guldi, D. M.; Torres, T. *Chem. Rev.* **2010**, *110*, 6768–6816. (c) Guldi, D. M.; Rahman, G. M. A.; Sgobba, V.; Ehli, C. *Chem. Soc. Rev.* **2006**, *35*, 471–487. (d) Fukuzumi, S.; Guldi, D. M. In *Electron Transfer in Chemistry*; Balzani, V., Ed.; Wiley-VCH: New York, 2001; Vol. 2, pp 270−337.

(4) Satake, A.; Kobuke, Y. *Org. Biomol. Chem.* **2007**, *5*, 1679–1691.

(5) (a) Sessler, J. L.; Lawrence, C. M.; Jayawickramarajah, J. *Chem. Soc. Rev.* **2007**, *36*, 314–325. (b) D'Souza, F.; Ito, O. *Coord. Chem. Rev.* **2005**, *249*, 1410–1422. (c) D'Souza, F.; Ito, O. *Chem. Commun.* **2009**, 4913–4928. (d) El-Khouly, M. E.; Ito, O.; Smith, P. M.; D'Souza, F. *J. Photochem. Photobiol. C* **2004**, *5*, 79–104.

(6) (a) Fukuzumi, S. *Org. Biomol. Chem.* **2003**, *1*, 609–620. (b) Fukuzumi, S. *Bull. Chem. Soc. Jpn.* **2006**, *79*, 177–195. (c) Fukuzumi, S. *Phys. Chem. Chem. Phys.* **2008**, *10*, 2283–2297. (d) Fukuzumi, S.; Kojima, T. *J. Mater. Chem.* **2008**, *18*, 1427–1439. (e) Fukuzumi, S.; Honda, T.; Ohkubo, K.; Kojima, T. *Dalton Trans.* **2009**, 3880–3889.

(7) Treibs, A.; Kreuzer, F. H. *Liebigs Ann. Chem.* **1968**, *718*, 208–223.

(8) Haugland, R. P. *Handbook of Fluorescent Probes and Research Chemicals*, 6th ed.; Molecular Probes: Eugene, OR, 1996.

(9) Loudet, A.; Burgess, K. *Chem. Rev.* **2007**, *107*, 4891–4932.

(10) (a) Kennedy, D. P.; Kormos, C. M.; Burdette, S. *J. Am. Chem. Soc.* **2009**, *131*, 8578–8586. (b) Rosenthal, J.; Lippard, S. *J. Am. Chem. Soc.* **2010**, *132*, 5536–5537.

(11) (a) Lee, Y. C.; Hupp, J. T. *Langmuir* **2010**, *26*, 3760–3765. (b) Godoy, J.; Vives, G.; Tour, J. M. *Org. Lett.* **2010**, *12*, 1464–1467.

(12) Nierth, A.; Kobitski, A. Y.; Nienhaus, G. U.; Jäschke, A. *J. Am. Chem. Soc.* **2010**, *132*, 2646–2654.

(13) Karolin, J.; Johansson, L. B.-A.; Strandberg, L.; Ny, T. *J. Am. Chem. Soc.* **1994**, *116*, 7801–7806.

(14) (a) Imahori, H.; Norieda, H.; Yamada, H.; Nishimura, Y.; Yamazaki, I.; Sakata, Y.; Fukuzumi, S. *J. Am. Chem. Soc.* **2001**, *123*, 100–110. (b) Hattori, S.; Ohkubo, K.; Urano, Y.; Sunahara, H.; Tetsuo Nagano, T.; Wada, Y.; Tkachenko, N. V.; Lemmetyinen, H.; Fukuzumi, S. *J. Phys. Chem. B* **2005**, *109*, 15368–15375.

(15) (a) Whited, M. T.; Djurovich, P. I.; Roberts, S. T.; Durrell, A. C.; Schlenker, C. W.; Bradforth, S. E.; Thompson, M. E. *J. Am. Chem. Soc.* **2011**, *133*, 88–96. (b) Lazarides, T.; McCormick, T. M.; Wilson, K. C.; Lee, S.; McCamant, D. W.; Eisenberg, R. *J. Am. Chem. Soc.* **2011**, *133*, 350–364. (c) Allik, T. H.; Hermes, R. E.; Sathyamoorthi, G.; Boyer, J. H. *Proc. SPIE-Int. Soc. Opt. Eng.* **1994**, *2115*, 240–248.

(16) (a) D'Souza, F.; Smith, P. M.; Zandler, M. E.; McCarty, A. L.; Itou, M.; Araki, Y.; Ito, O. *J. Am. Chem. Soc.* **2004**, *126*, 7898–7907. (b) Wijesinghe, C. A.; El-Khouly, M. E.; Blakemore, J. D.; Zandler, M. E.; Fukuzumi, S.; D'Souza, F. *Chem. Commun.* **2010**, *46*, 3301–3303. (c) Wijesinghe, C. A.; El-Khouly; Subbaiyan, N. K.; Supur, M.; Zandler, M. E.; Ohkubo, K.; Fukuzumi, S.; D'Souza, F. *Chem.—Eur. J.* **2011**, *17*, 3147–3156.

(17) (a) Liu, J.-Y.; El-Khouly, M. E.; Fukuzumi, S.; Ng, D. K. P. *Chem. Asian J.* **2011**, *6*, 174–179. (b) Liu, J.-Y.; El-Khouly, M. E.; Fukuzumi, S.; Ng, D. K. P. *Chem.—Eur. J.* **2011**, *17*, 1605–1613.

(18) (a) Gorman, A.; Killoran, J.; O'Shea, C.; Kenna, T.; Gallagher, W. M.; O'Shea, D. F. *J. Am. Chem. Soc.* **2004**, *126*, 10619–10631. (b) Hall, M. J.; McDonnell, S. O.; Killoran, J.; O'Shea, D. F. *J. Org. Chem.* **2005**, *70*, 5571–5578.

(19) (a) Loudet, A.; Burgess, K. *Chem. Rev.* **2007**, *107*, 4891–4932. (b) Li, F.; Yang, S. I.; Ciringh, T.; Seth, J.; Martin, C. H.; Singh, D. L.; Kim, D.; Birge, R. R.; Bocian, D. F.; Holten, D.; Lindsey, J. S. *J. Am. Chem. Soc.* **1998**, *120*, 10001–10017. (c) Tasior, M.; O'Shea, D. F. *Bioconjugate Chem.* **2010**, *21*, 1130–1133.

(20) (a) Palma, A.; Tasior, M.; Frimannsson, D. O.; Vu, T. T.; Meallet-Renault, R.; O'Shea, D. F. *Org. Lett.* **2009**, *11*, 3638–3641. (b) Murtagh, J.; Frimannsson, D. O.; O'Shea, D. F. *Org. Lett.* **2009**, *11*, 5386–5389.

(21) McDonnell, S. O.; Hall, M. J.; Allen, L. T.; Byrne, A.; Gallagher, W. M.; O'Shea, D. F. *J. Am. Chem. Soc.* **2005**, *127*, 16360–16361.

(22) Flavin, K.; Lawrence, K.; Bartelmess, J.; Tasior, M.; Navio, C.; Bittencourt, C.; O'Shea, D. F.; Guldi, D. M.; Giordani, S. *ACS Nano* **2011**, *5*, 1198–1206.

(23) (a) Xie, Q.; Perez-Cordero, E.; Echegoyen, L. *J. Am. Chem. Soc.* **1992**, *114*, 3978–3980. (b) Guldi, D. M. *Chem. Soc. Rev.* **2002**, *31*, 22–36. (c) El-Khouly, E. M.; Han, K.-J.; Kay, K.-Y.; Fukuzumi, S. *ChemPhysChem* **2010**, *11*, 1726–1734.

(24) Araki, Y.; Chitta, R.; Sandanayaka, A. S. D.; Langenwalter, K.; Gadde, S.; Zandler, M. E.; Ito, O.; D'Souza, F. *J. Phys. Chem. C* **2008**, *112*, 2222–2229.

(25) *Electrochemical Methods: Fundamentals and Applications*, 2nd ed.; Bard, A. J., Faulkner, L. R., Eds.; John Wiley: New York, 2001.

(26) (a) Rehm, D.; Weller, A. *Isr. J. Chem.* **1970**, *8*, 259–271. (b) Mataga, N.; Miyasaka, H. In *Electron Transfer*; Jortner, J., Bixon, M., Eds.; John Wiley & Sons: New York, 1999; Part 2, pp 431−496.

(27) Frisch, M. J.; Trucks, G. W.; Schlegel, H. B.; Scuseria, G. E.; Robb, M. A.; Cheeseman, J. R.; Zakrzewski, V. G.; Montgomery, J. A.; Stratmann, R. E.; Burant, J. C, et al. *Gaussian 03*; Gaussian, Inc.: Pittsburgh, PA, 2003.

(28) For a general review on DFT applications of porphyrin−fullerene systems, see:Zandler, M. E.; D'Souza, F. *C. R. Chem.* **2006**, *9*, 960–981.

(29) (a) Marcus, R. A. *J. Chem. Educ.* **1968**, *45*, 356–358. (b) Marcus, R. A.; Sutin, N. *Biochim. Biophys. Acta* **1985**, *811*, 265–322. (c) Marcus, R. A. *Angew. Chem., Int. Ed. Engl.* **1993**, *32*, 1111–1121.

(30) (a) Gould, I. R.; Moser, J. E.; Armitage, B.; Farid, S. *J. Am. Chem. Soc.* **1989**, *111*, 1917–1919. (b) Moser, C. C.; Keske, J. M.; Warncke, K.; Farid, R. S.; Dutton, P. L. *Nature* **1992**, *355*, 796–802. (c) Khan, S. I.; Oliver, A. M.; Paddon-Row, M. N.; Rubin, Y. *J. Am. Chem. Soc.* **1993**, *115*, 4919–4920. (d) Williams, R. M.; Zwier, J. M.; Verhoeven, J. W. *J. Am. Chem. Soc.* **1995**, *117*, 4093–4099.

(31) (a) Cannon, R. D. *Electron Transfer Reactions*; Butterworth: London, 1980. (b) Imahori, H.; Guldi, D. M.; Tamaki, K.; Yoshida, Y.; Luo, C.; Sakata, Y.; Fukuzumi, S. *J. Am. Chem. Soc.* **2001**, *123*, 6617–6628. (c) Adam, W.; Schönberger, A. *Chem. Ber.* **2006**, *125*, 2149–2153.

(32) The phosphorescence spectrum of ADP in the presence of CH_3I did not show any peaks in the range of 700−1200 nm, which suggests that the energy level of ^{3}ADP* lies at <1.0 eV.